Two-Step Formation of Methane–Propane Mixed Gas Hydrates in a Batch-Type Reactor

Tsutomu Uchida, Minoru Moriwaki, Satoshi Takeya, Ikuko Y. Ikeda, Ryo Ohmura, Jiro Nagao, Hideki Minagawa, Takao Ebinuma, Hideo Narita, Kazutoshi Gohara, and Shinji Mae
Institute for Energy Utilization, National Institute of Advanced Industrial Science and Technology (AIST), 2-17-2-1 Tsukisamu-higashi, Toyohira-ku, Sapporo 062-8517, Japan

Vapor compositions of methane and propane mixed gas in a batch-type reactor were measured by gas chromatography during hydrate crystallization at 274 K with molar ratios of propane below 10 vol %. The volume ratio of propane in the vapor decreased as the hydrate crystallization progressed. When the initial propane concentration was between 4 and 8 vol %, rapid gas consumption occurred for about 1 h, causing an initial pressure drop, and after a temporary stabilization of the pressure, a second pressure drop occurred; that is, hydrate crystallization occurred in two steps. X-Ray diffraction and Raman spectroscopic analyses on samples taken from the reactor during each step revealed that the structure II methane–propane mixed gas hydrates crystallized in the first step, and structure I methane hydrates in the second step. This process was observed only when the partial pressure of methane was above the equilibrium pressure of methane hydrate at the end of the first step. © 2004 American Institute of Chemical Engineers *AIChE J,* 50: 518–523, 2004

Keywords: methane-propane hydrate, batch-type reactor, crystallographic structure, second induction time

Introduction

Because deep-sea sediments and permafrost contain huge amounts of natural gases stored in crystalline hydrates, researchers have recognized that gas hydrates could be an unconventional natural-gas energy resource (Dallimore and Collett, 1999). In addition, a given volume of hydrates contains more than 150 times as much natural gas than the gas phase at standard temperature and pressure. Thus, gas hydrates are also a promising material for gas storage.

Light hydrocarbon molecules, such as methane (CH_4), ethane (C_2H_6), and propane (C_3H_8), are major components of natural gas. Most light hydrocarbons are known to form gas hydrates. Of the two crystalline structures for gas hydrates, CH_4 hydrate and C_2H_6 hydrate form structure I hydrates (sI), and larger guest molecules such as C_3H_8 form structure II hydrates (sII) (see, for example, Clausen, 1951; Stackelberg and Muller, 1954; Gutt et al., 2000). As is the case with all hydrates, gas hydrates are stable only under high-pressure and low-temperature conditions.

For mixtures of such gases, both the equilibrium conditions and the structures of the resulting gas hydrates are rather complicated, sensitive functions of the conditions of the gas compositions. For example, gas hydrates formed from gas mixtures of CH_4 with small amounts of C_3H_8 are expected to form sII at lower pressures than the pure CH_4 hydrate (van der Waals and Platteeuw, 1959). In this hydrate, C_3H_8 molecules occupy only the large cage, whereas CH_4 molecules exist in the remaining cages (both small and large cages) of the sII hydrate, a structure that was predicted from solid solution theory (van der Waals and Platteeuw, 1959) and confirmed by NMR measurements (Ripmeester and Ratcliffe, 1988). Mixtures of CH_4 and C_2H_6 are also found to form both sI and sII hydrate, depending on the vapor composition in equilibrium with the

Correspondence concerning this article should be addressed to T. Uchida at t.uchida@aist.go.jp.
Current address of: M. Moriwaki and K. Gohara, Faculty of Engineering, University of Hokkaido, Sapporo 060-8628, Japan; S. Mae, Asahikawa National College of Technology, 2-2-1-6 Shunkodai, Asahikawa 071-8142, Japan.

hydrate phase. This interesting phenomenon was predicted theoretically (Hendriks et al., 1996) and confirmed experimentally (Subramanian et al., 2000a,b; Ballard and Sloan, 2000; Uchida et al., 2002).

When such gas mixtures react with water in a batch-type reactor, the thermodynamic model predicts that the component with the greater driving force should crystallize faster than the other component. Thus, both the guest composition and the crystal structure are expected to change during hydrate formation. Even though hydrate samples have been prepared using such a batch-type reactor in many studies, this complicated process is not understood well enough to accurately know the physical properties of the sample. A better understanding of the formation of mixed gas hydrates in a batch-type reactor may also help us to determine the feasibility of using gas hydrates for natural gas storage and transportation.

For the present study, we used a high-speed gas chromatograph (GC) to measure the composition change in the vapor phase containing CH_4 and C_3H_8 gases during hydrate formation. In agreement with thermodynamics, the final vapor compositions were further enriched in CH_4 over those in the initial compositions. However, GC measurements and the drops in pressure indicated that the mixed-gas hydrate formation had two steps. The two-step formation process was recognized by a temporary period of nearly constant pressure after the vapor composition became rich in CH_4. When the initial C_3H_8 concentration was between 4 and 8 vol %, the two constant-pressure periods were clearly observed. Both X-ray diffraction (XRD) and Raman spectroscopic analyses were done on several CH_4-C_3H_8 hydrate samples to characterize the hydrates in each step of the two-step formation process. CH_4 and C_3H_8 mixed gas hydrate with structure II formed at the first step, whereas almost pure CH_4 hydrates with structure I formed in the second step. These findings show the importance of sample characterization for the mixed-gas hydrate studies when samples are prepared using a batch-type reactor.

Experimental Methods

Our experimental apparatus for forming mixed gas hydrate was previously used for a study of CH_4 hydrate formation (Uchida et al., 1999). This apparatus consists of a high-pressure, low-temperature reaction vessel with type T thermocouples, a gas inlet–outlet with pressure gauge (Nagano Keiki Seisakusho type KH15), and a temperature-controlled bath with cold media. The reaction temperature was fixed at 274.0 ± 0.1 K. The total volume of the reaction vessel was 232.2 ± 0.2 cm^3, and the contents could be stirred at up to 1000 rpm. To avoid variations in sample properties due to variations in stirring rate (Narita and Uchida, 1996), we fixed the stirring rate at approximately 500 rpm.

We describe the gas compositions using the volume ratio X_i, where i is $C1$ to indicate CH_4 and i is $C3$ for C_3H_8. These were measured using an on-line high-speed GC (AREA model MC-200) calibrated using standard CH_4-C_3H_8 mixed gases (supplied by Hokkaido Air Water Co.). To accurately measure the vapor composition, we did four GC measurements, each taking less than 1 min, over a 5-min period and averaged the results to reduce any contamination effects. Over this 5-min period, the total pressure decreased by about 0.5%. The gas composition in the hydrate was also obtained by the GC measurement of the gas decomposed from the hydrate sample. The uncertainty of GC measurements was estimated to be within 5 vol %.

Deionized, distilled water (conductivity of 18.2 M$\Omega \cdot$ cm) and purified gases (99.995 vol % for CH_4 and 91.2 vol % for C_3H_8) were used in the experiments. GC measurements indicated that the C_3H_8 gas included 6.7 vol % of CH_4 and 2.1 vol % of C_2H_6. A small amount of C_2H_6 (approximately 0.7 mol %) in a mixture with CH_4 is known to change the structure (Subramanian et al., 2000b); however, because the complete mixture is at least 90 vol % CH_4, the 2.1 vol % of C_2H_6 in C_3H_8 gas becomes at most 0.2 vol % of the complete mixture. This amount should not significantly alter the structure. To check this potential problem, we performed a reference experiment using pure CH_4 gas and a standard CH_4-C_3H_8 mixed gas, with a C_3H_8 concentration of 9.91 vol % in CH_4. Air in the water and dead space of the reaction vessel was removed by pumping for several minutes with a diaphragm-type vacuum pump prior to the pressurization.

The reaction vessel was then cooled to the experimental temperature and pressurized by the mixed gas to a specific pressure. After both pressure and temperature stabilized, the initial gas composition was measured. Then the mixture was stirred. While the formation reaction proceeded, the pressure decreased.

To determine the crystal types and compositions at each step, we characterized the samples formed in the high-pressure vessel at each step by using XRD and Raman spectroscopy. The sample from the first step was prepared as follows: after the hydrate had crystallized for several minutes, the stirrer was stopped and the high-pressure vessel was soaked in a liquid nitrogen bath. This quench process prevented any further hydrate growth in the vessel because it froze the free water and essentially stopped hydrate growth. When the temperature of the sample decreased below 190 K, the free gas in the vessel was released and the sample was taken out. This cooling process was necessary to prevent hydrate dissociation when samples were removed from the vessel at atmospheric pressure. The sample was then stored in the container at approximately 80 K for the spectroscopic analyses. After all hydrate crystallization ceased, the second-step sample was taken from the vessel using the same sampling procedures as those in the first step. With this procedure, the sample for the spectroscopic analyses included both hydrates and ice. The crystallographic structures in the sample were identified using XRD on finely powdered hydrate, and the gas components in the hydrate were measured using Raman spectroscopy. The XRD and Raman spectroscopy measurements were not done on the same sample, but they were picked from the same region in the vessel. Further details of the measurement procedures are in Uchida et al. (2002).

The experimental setup of the Raman spectroscopic measurements was similar to that used in our previous study (Uchida et al., 1999). The specimen was set below the objective lens and the scattered radiation was collected through a 200-μm slit with 180-degree geometry. With a $\times 40$ objective lens, the magnification of the system was approximately 10^3. The incident laser-beam was focused to a diameter of about 5-μm on the specimen. This setup allowed us to distinguish hydrate particles of sizes exceeding 5 μm. The temperature of the specimen was maintained at approximately 150 K during measurements by controlling the flow speed of N_2 gas that

Table 1. Experimental and Equilibrium Conditions of Methane–Propane Mixed Gas Hydrates

X^0_{C3} [vol %]	P^0 [MPa]	P^d [MPa]	P^f [MPa]	X^f_{C3} [vol %]
8	6.9	0.57	3.2	<0.1
6	6.4	0.65	2.5	<0.1
4	6.9	0.78	2.5	<0.1
2	6.9	1.0	1.8	<0.1
0.5	5.8	1.7	2.5	<0.1
0.33	5.8	1.9	2.5	<0.1
9	2.8	0.54	0.6	1.4

Note: X^0_{C3} and X^f_{C3} are the initial and final propane concentrations in the vapor phase. Similarly, P^0 and P^f are the initial and final total pressures in the vessel. P^d is the equilibrium pressure for the gas mixture of X^0_{C3} at 274 K, which was calculated using CSMHYD (Sloan, 1998).

vaporized from liquid nitrogen. For calibration, the line shape of neon emission lines indicated that the wave number of peak positions were determined within ± 1 cm^{-1}.

The crystal structures were determined using a Cu-Kα X-ray (40 kV, 250 mA; Rigaku model Rint-2000). The hydrate samples were put in a quartz-glass capillary cell (Hilgenberg; 2.0-mm diameter, 0.01-mm thick) that was put on top of the goniometer. These measurements were done at 113.0 $\pm$ 1.0 K by blowing cold, dry nitrogen gas at atmospheric pressure around the sample. Due to the low temperature, dissociation of the hydrate samples during the measurements was negligible. Further details of the XRD measurement procedures for gas hydrates are in Takeya et al. (2003).

Results and Discussion

The CH_4-C_3H_8 gas composition and the partial pressures of CH_4 (P_{C1}) and C_3H_8 (P_{C3}) changed during the hydrate formation. The initial fraction of C_3H_8 (X_{C3}) was kept below 10 vol % to prevent condensation of C_3H_8 during the experiments. When the hydrate started to form, the total pressure decreased with time due to the gas consumption for hydrate crystallization. The experimental conditions in the present study are summarized in Table 1. This table also includes the equilibrium pressure at a given temperature and the initial conditions in the vapor phase.

Figure 1 shows the partial pressure change of P_{C1} and P_{C3}, with time for an initial vapor composition X_{C3} = 6 vol %. In this experiment, P_{C3} suddenly drops when the hydrate first forms, and steadily falls to zero within 3 h. The value of P_{C3} after 1 hour is much lower than the equilibrium pressure of pure C_3H_8 hydrate (0.2 MPa at 274 K). After P_{C3} goes below 0.01 MPa at about 1 h, P_{C1} becomes steady at about 4.4 MPa, a pressure that is much higher than 2.8 MPa, the equilibrium pressure of pure CH_4 hydrate at 274 K. Thus, hydrate continues to form and P_{C1} falls to the equilibrium pressure. The intermediate plateau of pressure typically lasts for several minutes to several hours, depending on X_{C3}. Hereafter, we call the period of this plateau the "second" induction period to distinguish it from the normally used induction period that occurs prior to hydrate formation. In several experiments, in which X_{C3} ranged from 4 vol % to 8 vol %, we observed such a two-step formation process.

The pressure difference between the initial and the equilibrium pressure of CH_4 ranged from 3.9 MPa to 6.3 MPa, as shown in Table 1. Of these pressures, the larger initial pressures were used with larger C_3H_8 concentrations, X_{C3}. The

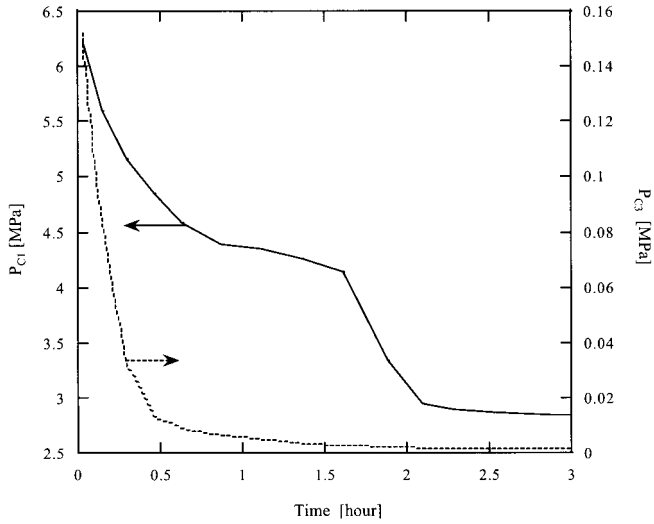

Figure 1. Typical partial pressures of CH_4 (P_{C1}) and C_3H_8 (P_{C3}) during hydrate crystallization.

Experimental temperature was 274 K and the initial pressure was 6.5 MPa. The initial concentration of C_3H_8 in the vapor phase was 6 vol %.

final pressure depended on the experimental running time, but it tended to be lower than the equilibrium pressure of pure CH_4 hydrates.

Figure 2 shows the XRD patterns of samples from (a) the first-step and (b) second-step. Each diffraction peak is assigned to one of the peaks from hydrate sI, sII, or hexagonal ice (*). Every diffraction peak fits well to a diffraction peak of sI, sII, or hexagonal ice. This figure shows that only sII hydrates formed at the first step, whereas a mixture of type sI and sII

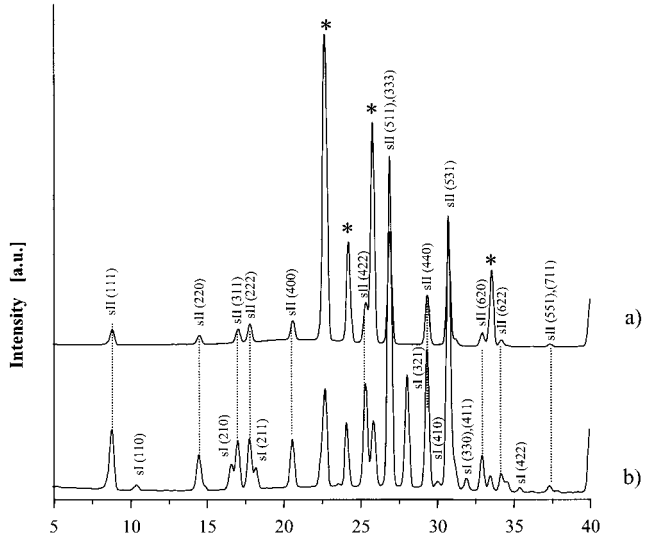

Figure 2. XRD patterns from samples removed during (a) the first step and (b) second step.

Experimental temperature was 274 K and the initial pressure was 7 MPa. The initial concentration of C_3H_8 in the vapor phase was 6 vol %. Each diffraction peak is assigned to hydrate structure I (sI), structure II (sII), or hexagonal ice (*). Crystal plane indices are also shown. Dotted lines connect the sII peaks for both samples.

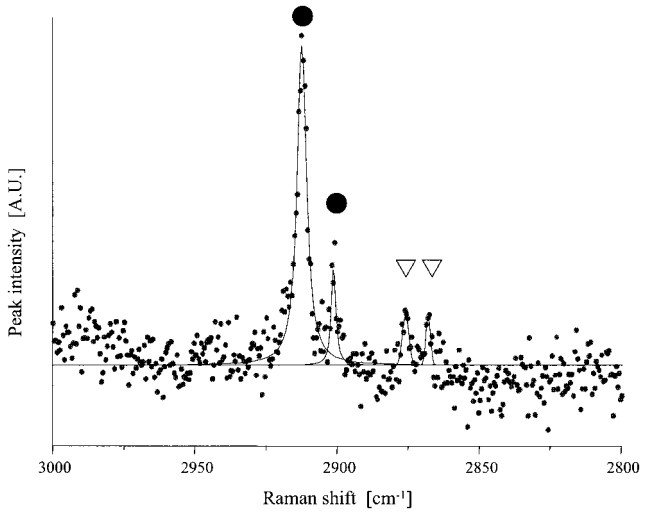

Figure 3. C–H stretching-mode Raman spectra from the same first-step sample that was used for Figure 2a: solid circles and open triangles indicate the CH_4 peaks and C_3H_8 peaks, respectively.

formed at the second step. Of the two pure hydrates here, the sI hydrate can only be CH_4 hydrate. The Raman spectroscopic measurements did not give any evidence of C_2H_6 molecules included in the hydrate crystals. Therefore, we conclude that the sI hydrate in the second step is CH_4 hydrate.

Raman spectroscopic analyses on these samples supports the conclusion obtained from XRD analyses. Figure 3 shows the C–H stretching mode of encaged guest molecules obtained from the first-step sample. Two large peaks at approximately 2905 cm^{-1} and 2915 cm^{-1} indicate CH_4 molecules encaged in large cages and small cages, respectively (Sum et al., 1997; Uchida et al., 1999; Subramanian and Sloan, 2002). Two small peaks at approximately 2865 cm^{-1} and 2876 cm^{-1} are from the C_3H_8 molecules in the hydrate lattice. These peaks have a relatively low signal-to-noise level due to the small amount of C_3H_8; nevertheless, the correlation coefficient of the curve fitting shown in Figure 3 is about 0.97. To help us determine if these peaks are from C_3H_8 in the hydrate lattice or if they are from liquid C_3H_8, we measured the Raman spectra of liquid C_3H_8 in the same wave-number region (Figure 4a) and compared it with that from pure C_3H_8 hydrate (Figure 4b). As shown in these figures, the largest peak at 2875 cm^{-1} in the liquid C_3H_8 phase was separated into two peaks (2870 cm^{-1} and 2880 cm^{-1}) in the hydrate lattice. These peaks are good indicators of the C_3H_8 molecules enclathrated in the hydrate lattice. The peaks from the mixed-gas hydrate sample are small but obviously different from the peaks observed for the liquid phase. These spectra indicate that the sample contains both CH_4 and C_3H_8 molecules in the hydrate lattice, that is, the sample is the CH_4-C_3H_8 mixed gas hydrate, which is sII. The C_3H_8 peaks in the mixed-gas hydrate sample are about 5 cm^{-1} lower than those observed in pure C_3H_8 hydrate (Figure 4b). This difference might be caused by the influence of CH_4 molecules in neighboring cages.

Because the boiling point of C_3H_8 is about 230 K at atmospheric pressure, some C_3H_8 in the vapor phase might condense during the quenching process. This likely has no effect on the second-step sample because the C_3H_8 pressure was very small in the vapor phase during quenching as indicated by the values in the last two columns of Table 1. Even for the first-step samples, the amount of condensed C_3H_8 should be insignificant. If the condensed C_3H_8 reacted with ice during the sample storage, it could form the sII hydrate of pure C_3H_8. But this process is expected to be slow. Furthermore, if such crystals had existed in our sample, we would have distinguished them with our microscopic Raman spectra as regions without CH_4. However, in all regions of the sample that we tested, there were signals from CH_4 molecules. Also, we did not find any regions with the distinguishing peaks showing liquid C_3H_8 (see the inset in Figure 3). Therefore, we assume that there was no liquid C_3H_8 in the samples.

Figure 5 shows the Raman spectra obtained from the second-step sample. In agreement with Figure 3, Figure 5a shows the existence of CH_4-C_3H_8 mixed gas hydrates. The mixed gas hydrate in Figure 5a likely formed at the first step. In Figure 5b, we show an example from a sample with no C_3H_8 peaks and CH_4 peak intensities different from those in Figure 5a; both of these features suggest pure CH_4 hydrates. Based on these spectroscopic analyses, we conclude that CH_4-C_3H_8 mixed gas hydrates (sII) formed at the first step, and that pure CH_4 hydrates (sI) formed at the second step. This is consistent with our analysis of the GC measurements. In the case of XRD measurements, about 10×1 mm^2 of the X-ray beam was radiated to the sample. Therefore, XRD results confirmed that both sI and sII hydrates coexisted in the radiation area of X-ray beam.

To determine the cause of the two-step process, we studied the mixed gas hydrates at the lower initial pressure of about 3 MPa. Consistent with the first step of the previous, higher-pressure experiment, both partial pressures decreased with time. In particular, P_{C3} decreased to approximately 0.01 MPa within 1 h and became constant; here, P_{C1} was below the

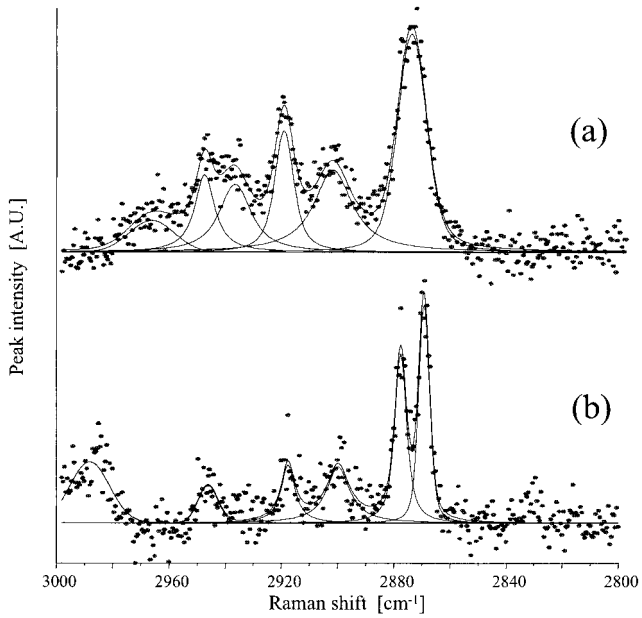

Figure 4. C–H stretching-mode Raman spectra of (a) liquid C_3H_8 and (b) pure C_3H_8 hydrate.

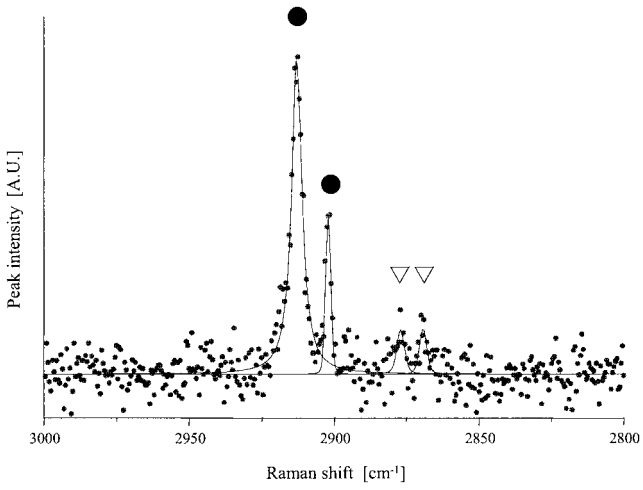

(a)

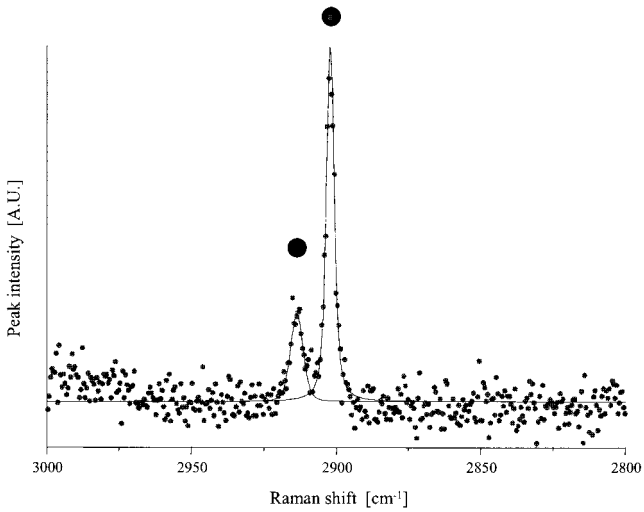

(b)

Figure 5. Raman spectra measured on samples taken during the second step from two different locations in the same specimen.

The specimen was the same as that used for Figure 2b. Symbols are same as those in Figure 3.

dissociation pressure of pure CH_4 hydrates and there was no indication of the two-step process, such as the second induction period. Thus, comparison of these experiments indicates that the second step resulted from the formation of CH_4 hydrate in the system.

Therefore, our data indicate the following crystallization sequence. At the first step of the formation process, both CH_4 and C_3H_8 molecules are enclathrated into mixed gas hydrates because both partial pressures are high enough to form hydrate. In this step, C_3H_8 molecules are preferentially encaged in the hydrate crystals, which reduces P_{C3} in the vapor phase to below 0.01 MPa. If P_{C1} in the vapor phase remains higher than the dissociation pressure of pure CH_4 hydrate after the first step, then the pure CH_4 hydrates can form, thus causing the second step. The period of time between these steps depends on the initial composition in the vapor phase.

Two-step processes during the hydrate formation also occur in the Xe-THF system (Moudrakovski et al., 2001) and in the CH_4-THF system (Seo et al., 2003). For the Xe-THF system, Xe hydrate forms on THF hydrate surfaces at temperatures below the ice point, which indicates fast formation of the semistable Xe hydrate (sII) and the subsequent growth of either the stable Xe hydrate (sI) or Xe THF hydrate (sII). This system is slightly different from the present study; that is, THF hydrate (sII) was present initially and served as a template to induce the semistable sII Xe hydrate. For the CH_4-THF study, on the other hand, the formation conditions were similar to those in the present study. NMR analysis revealed that the stoichiometric THF-CH_4 hydrate formed at the first step and the pure CH_4 hydrate formed at the second step. Seo et al. (2003) found a two-step formation process in the water-rich solution system, whereas a single step occurred in the stoichiometric THF solution system. This finding indicates that the second step for CH_4-hydrate formation requires free water and excess CH_4 gas, a finding that is consistent with the present study. One difference is that THF forms stoichiometric hydrates with CH_4 in the small cages of sII, whereas CH_4-C_3H_8 mixed gas forms nonstoichiometric hydrates that include CH_4 molecules in both large and small cages of the sII crystal. The critical parameter of the CH_4-hydrate formation is the partial pressure of CH_4 at the end of the first step, after most of the C_3H_8 has been consumed. We now consider the mechanism of the two-step process for mixed-gas hydrates under nonstoichiometry.

The gas component with the lower dissociation pressure at a given temperature, hereafter the "milder" hydrate former, has the greater driving force for crystallization, and hence should crystallize faster than the other component. Thus, the vapor composition will become depleted of the milder hydrate former. Here, P_{C3} at the end of the first step was smaller than the dissociation pressure of pure C_3H_8 hydrate. This implies that the formation of the mixed-gas hydrate in the first step was strongly affected by CH_4 molecules; that is, a sufficient amount of CH_4 in vapor phase allowed formation of mixed gas hydrate together with the consumption of C_3H_8 at relatively low C_3H_8 pressures. Therefore, the first step of hydrate formation mostly includes the milder hydrate former (C_3H_8 here), but this step is also influenced by the other component. The appearance of the second step of the hydrate formation process in that system will depend on the conditions of the remaining hydrate former (CH_4 here).

The existence of a second induction period at the transition between the first and second steps has interesting implications for the hydrate formation process. Generally, the induction period is believed to be the period for nucleation of hydrate crystals to occur. The composition of the vapor phase at the second induction period was almost pure CH_4; thus, the second induction period is assumed to be that for CH_4 hydrate formation. We found that the duration of the second induction period varied with the initial composition of the vapor phase. When the initial C_3H_8 concentration was 4 vol %, the second induction period was approximately 3 h. However, when the concentration was 8 vol %, the second induction period was less than 5 min and appeared as a shoulder of the P_{C1} time curve. The reason for the variation of the second induction period has not been revealed, but one possibility is that nucleation for the second step is promoted by hydrate surfaces from the first step with a nucleation rate that increases with the hydrate surface

area. Moudrakovski et al. (2001) showed that sII THF hydrate acts as a template for sII Xe hydrate; they found that THF hydrate led to a shorter induction period compared to that for Xe hydrate on ice. Thus, the studies just cited are consistent with ours and show, as expected, that the existence of hydrate crystals in the system helps to nucleate other hydrate crystals. When the initial C_3H_8 concentration X_{C3} was larger, the volume of the hydrates during the first step was greater. This provides more heterogeneous nucleation sites for sII hydrate crystals; this can explain why a greater initial propane concentration had a shorter second induction period.

Based on our experimental results, we summarize hydrate formation from CH_4 and C_3H_8 gases mixed with water in a batch-type reactor. Both CH_4 and C_3H_8 molecules were enclathrated into the sII hydrate crystals after hydrate began crystallizing. C_3H_8 molecules were preferentially removed from the vapor at this step and, thus, the composition of the vapor gradually became more CH_4-rich. This first step continued until the concentration of C_3H_8 in the vapor phase was nearly zero. When the initial concentration of C_3H_8 in the mixed gas was below 8 vol %, the first step usually ended within 1 h. If the partial pressure of CH_4 remained higher than the dissociation pressure of pure CH_4-hydrate at the sample temperature, then sI CH_4-hydrate started to crystallize after an interval in which no gas consumption could be detected. The interval of this interruption, which we called the second induction period, depended on the initial C_3H_8 concentration in the vapor phase. This two-step process was confirmed by XRD and Raman spectroscopy using quenched samples taken from each step. These findings point out the importance of sample characterization when mixed gas hydrates are formed in a batch-type reactor. In addition, the results indicate that the method might be useful for gas separation processes because the partial pressure of C_3H_8 became far lower than the dissociation pressure of the C_3H_8 hydrate at a given temperature.

Acknowledgments

A part of this work was supported financially by the NEDO-grant entitled "Studies on Energy Translation Technology using Clathrate Compounds" (00B60016d) and by the international joint project entitled "Research and Development on Natural Gas System Utilizing Gas Hydrate Technology" in collaboration with the Institute of Applied Energy. Dr. K. Haraguchi kindly provided us the high-quality distilled and deionized water. We greatfully acknowledge Mr. S. Date and Ms. M. Akaike-Konishi for their support of the experiments.

Literature Cited

Ballard, A. L., and E. D. Sloan, Jr., "Structural Transitions in Methane + Ethane Gas Hydrates—Part II: Modeling Beyond Incipient Conditions," *Chem. Eng. Sci.,* **55**, 5773 (2000).

Claussen, W. F., "Suggested Structure of Water in Inert Gas Hydrates," *J. Chem. Phys.,* **19**, 259 (1951).

Dallimore, S. R., and T. S. Collett, "Regional Gas Hydrate Occurrences, Permafrost Conditions, and Cenozoic Geology, Mackenzie Delta Area," *Scientific Results from JAPEX/JNOC/GSC Mallik 2L-38 Gas Hydrate Research Well, Mackenzie Delta, Northwest Territories, Canada*, S. R. Dallimore, T. Uchida, and T. S. Collett, eds., *Geol. Surv. Can. Bull.,* **544**, 31 (1999).

Gutt, C., B. Asmussen, W. Press, M. R. Johnson, Y. P. Handa, and J. S. Tse, "The Structure of Deuterated Methane-Hydrate," *J. Chem. Phys.,* **113**, 4713 (2000).

Hendriks, E. M., B. Edmonds, R. A. S. Moorwood, and R. Szczepanksi, "Hydrate Structure Stability in Simple and Mixed Hydrates," *Fluid Phase Equilib.,* **117**, 193 (1996).

Moudrakovski, I. L., C. I. Ratcliffe, and J. A. Ripmeester, "Probing Transient Hydrate Structures with Hyperpolarized ^{129}Xe NMR Spectroscopy: A Metastable Structure II Hydrate of Xe," *Angew. Chem. Int. Ed.,* **40**, 3890 (2001).

Narita, H., and T. Uchida, "Studies on Formation/Dissociation Rates of Methane Hydrates," *Proc. Int. Conf. on Natural Gas Hydrates*, Toulouse France, p. 191 (1996).

Ripmeester, J. A., and C. I. Ratcliffe, "Low-Temperature Cross-Polarization/Magic Angle Spinning 13C NMR of Solid Methane Hydrates: Structure, Cage Occupancy, and Hydration Number," *J. Phys. Chem.,* **92**, 337 (1988).

Seo, Y.-T., H. Lee, I. L. Moudrakovski, and J. A. Ripmeester, "Phase Behavior and Structural Characterization of Coexisting Pure and Mixed Clathrate Hydrates," *Chem Phys Chem.,* **4**, 379 (2003).

Sloan, E. D., Jr., *Clathrate Hydrates of Natural Gases*, 2nd ed. Revised and Expanded, Chap. 6, Marcel Dekker, New York (1998).

Stackelberg, M. V., and H. R. Muller, "Feste Gashydrate II, Struktur und Raumchemie," *Z. Elektrochem.,* **58**, 25 (1954).

Subramanian, S., R. A. Kini, S. F. Dec, and E. D. Sloan, Jr., "Evidence of Structure II Hydrate Formation from Methane + Ethane Mixtures," *Chem. Eng. Sci.,* **55**, 1981 (2000a).

Subramanian, S., R. A. Kini, S. F. Dec, and E. D. Sloan, Jr., "Structural Transitions in Methane + Ethane Gas Hydrates—Part I: Upper Transition Point and Applications," *Chem. Eng. Sci.,* **55**, 5763 (2000b).

Subramanian, S., and E. D. Sloan, Jr., "Trends in Vibrational Frequencies of Guests Trapped in Clathrate Hydrate Cages," *J. Phys. Chem. B.,* **106**, 4348 (2002).

Sum, A. K., R. C. Burruss, and E. D. Sloan, Jr., "Measurement of Clathrate Hydrates via Raman Spectroscopy," *J. Phys. Chem. B.,* **101**, 7371 (1997).

Takeya, S., Y. Kamata, T. Uchida, J. Nagao, T. Ebinuma, H. Narita, A. Hori, and T. Hondoh, "Coexistence of Structure I and II Hydrate Formed from a Mixture of Methane and Ethane Gases," *Can. J. Phys.,* **81**, 479 (2003).

Uchida, T., T. Hirano, T. Ebinuma, H. Narita, K. Gohara, S. Mae, and R. Matsumoto, "Raman Spectroscopic Determination of Hydration Number of Methane Hydrates," *AIChE J.,* **45**, 2641 (1999).

Uchida, T., S. Takeya, Y. Kamata, I. Y. Ikeda, J. Nagao, T. Ebinuma, H. Narita, O. Zatsepina, and B. A. Buffett, "Spectroscopic Observations and Thermodynamic Calculations on Clathrate Hydrates of Mixed Gas Containing Methane and Ethane: Determination of Structure, Composition and Cage Occupancy," *J. Phys. Chem. B.,* **106**, 12426 (2002).

Van der Waals, J. H., and J. C. Platteeuw, "Clathrate Solutions," *Adv. Chem. Phys.,* **2**, 1 (1959).

Manuscript received Oct. 21, 2002, and revision received June 2, 2003.